Integration of geometrical root system approximations in hydromechanical slope stability modelling

Schmaltz, Elmar; Van Beek, Rens V.; Bogaard, Thom; Steger, Stefan; Glade, Thomas

DOI
10.1007/978-3-319-53483-1_35

Publication date
2017

Document Version
Final published version

Published in
Landslides in Different Environments

Integration of Geometrical Root System Approximations in Hydromechanical Slope Stability Modelling

Elmar Schmaltz, Rens Van Beek, Thom Bogaard, Stefan Steger, and Thomas Glade

Abstract

Spatially distributed physically based slope stability models are commonly used to assess landslide susceptibility of hillslope environments. Several of these models are able to account for vegetation related effects, such as evapotranspiration, interception and root cohesion, when assessing slope stability. However, particularly spatial information on the subsurface biomass or root systems is usually not represented as detailed as hydropedological and geomechanical parameters. Since roots are known to influence slope stability due to hydrological and mechanical effects, we consider a detailed spatial representation as important to elaborate slope stability by means of physically based models. STARWARS/PROBSTAB, developed by Van Beek (2002), is a spatially distributed and dynamic slope stability model that couples a hydrological (STARWARS) with a geomechanical component (PROBSTAB). The infinite slope-based model is able to integrate a variety of vegetation related parameters, such as evaporation, interception capacity and root cohesion. In this study, we test two different approaches to integrate root cohesion forces into STARWARS/PROBSTAB. Within the first approach, the spatial distribution of root cohesion is directly related to the spatial distribution of land use areas classified as forest. Thus, each pixel within the forest class is defined by a distinct species related root cohesion value where the potential maximum rooting depth is only dependent on the respective species. The second method represents a novel approach that approximates the rooting area based on the location of single tree stems. Maximum rooting distance from the stem, maximum depth and shape of the root system relate to both tree species and external influences such as relief or soil properties. The geometrical

E. Schmaltz (✉) · S. Steger · T. Glade
Faculty of Geosciences, Geography and Astronomy, ENGAGE—Geomorphological Systems and Risk Research, University of Vienna, Vienna, Austria
e-mail: elmar.schmaltz@univie.ac.at

S. Steger
e-mail: stefan.steger@univie.ac.at

T. Glade
e-mail: thomas.glade@univie.ac.at

R. Van Beek
Faculty of Geosciences, Utrecht University, Utrecht, The Netherlands
e-mail: r.vanbeek@uu.nl

T. Bogaard
Faculty of Civil Engineering and Geoscience, Delft University of Technology, Delft, The Netherlands
e-mail: T.A.Bogaard@tudelft.nl

M. Mikoš et al. (eds.), *Advancing Culture of Living with Landslides*,
DOI 10.1007/978-3-319-53483-1_35

cone-shaped approximation of the root system is expected to represent more accurately the area where root cohesion forces are apparent. Possibilities, challenges and limitations of approximating species-related root systems in infinite slope models are discussed.

Keywords
Physical based modelling • Soil reinforcement • Root system approximation • Slope stability

Introduction

The stabilizing effect of vegetation on slopes was addressed in many studies (e.g. Sidle et al. 1985; Sidle and Ochiai 2006; Stokes et al. 2014). Plant roots are known to reinforce hillslopes by mechanically anchoring into the ground and extracting moisture out of the soil mantle (Stokes et al. 2008; Genet et al. 2008; Ghestem et al. 2011; Papathomas-Koehle and Glade 2013). Thereby, the above-ground (organic matter, stem, branches, leafs) and the below-ground biomass (roots) form a soil-plant continuum with the ground the plant is standing on. The negative pressure in the xylem that is induced by evaporation from the leafs, actuate the water extraction of roots from the surrounding soil material. Hence, plants have considerable effects on the hydrological balance of a landscape and are able to significantly increase the stability of the rooted soil mantle (Ghestem et al. 2011).

Several studies tackled the issues that affect the reinforcing potential of vegetation on a slope—in particular of root systems. For instance, Schwarz et al. (2012), Schmidt and Kazda (2002), Pollen and Simon (2005) and Danjon et al. (2002) highlighted the effects of different root systems and architectures on slope stability and on the Factor of Safety (FoS). Greenway (1987), Fan and Su (2008) and Meng et al. (2014) showed that the hydrological influences of forest stands on slopes have direct effects on the mechanical stability. Whereas, Multiple studies all over the globe (Ziemer 1981; Sidle 1991; Montgomery et al. 2000; Sidle and Ochiai 2006; Imaizumi et al. 2008) addressed the effects of tree stand removal and the reduction of stability due to decay of root systems of harvested trees.

Many modelling and simulation approaches attempted to quantify the effect of roots (Danjon et al. 2002; Van Beek et al. 2007; Schwarz et al. 2010, 2012; Thomas and Pollen-Bankhead 2010) and to implement stabilizing forces of roots into the Factor of Safety equation. However, vegetation in general and roots in particular appear to be rather underrepresented in physically based slope stability models (Schmaltz et al. 2016a).

In this study, we highlight the possibilities and drawbacks of a simple root system approximation and its implementation in a well-established hydromechanic slope stability model. Hereto, we compared three different land cover scenarios.

Study Area

The area of investigation is situated at the South-facing slope of the Walserkamm ridge within the Walgau valley in Vorarlberg, Austria. The area is delimited by the creeks Schnifiser Tobel to the East and Montanastbach to the West while ranging in altitude from 625 m.a.s.l. to 1971 m.a.s.l. (Fig. 1). Primarily consolidated morainic material covers the geological underground that is composed of alternating sandstone and claystone layers, partly interrupted by limestones (Friebe 2013). Particularly in the lower slope section between Düns and Montanast and as well in the Pfänder area

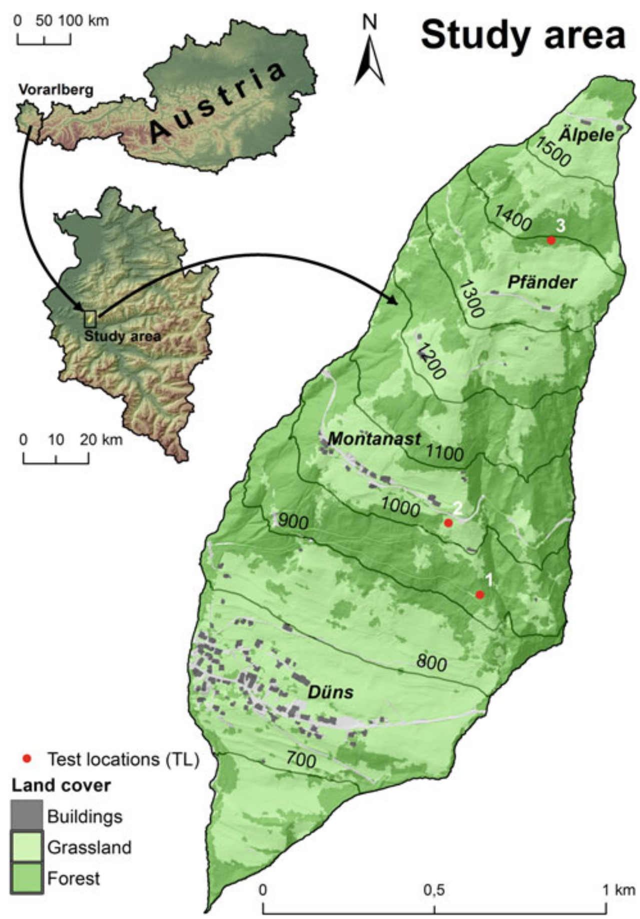

Fig. 1 Location and land cover of the study area

(Fig. 1), marls are widespread. Alpine pastures and timberland depict the land use of the area. A considerable amount of the forests are economically used conifer stands (spruces and firs), which are primarily located in steeper areas of the slopes. However, the species composition of the stands is under continuous change towards a higher diversity of deciduous trees and conifers. In this regard, the forested areas in the lower slope part around Düns and Montanast are mixed stands.

Under consideration of previous studies (Tilch 2014; Ruff and Czurda 2008), several field campaigns have been conducted to investigate the landslide dynamics of the area (Schmaltz et al. 2016a, b). In 1999, 14 landslides were triggered during an intense rainfall event. Although the exact time of failure can not be determined, personal communications with locals and archive data from the Torrent and Avalanche Control (WLV, Wildbach- und Lawinenverbauung) revealed that most of the mapped landslides of that period occurred on the 20th of May 1999.

Data

Digital Terrain Model (DTM)

We used a 1 × 1 m DEM that was obtained from LiDAR flights in 2004 and provided by the Federal State of Vorarlberg. The DEM was resampled to 2.5 m to ensure both, computational feasibility and an adequate level of detail for the approximation of the root systems.

Land Cover Data

Forested areas as well as buildings and sealed areas (roads, parking lots) were digitized, based on a RGB-orthophoto of 2001. It is assumed that the 2001 conditions remain until today. Stands of different tree species were not distinguished. All areas that were not assigned as 'forest' or 'sealed (buildings, roads)' were considered as grassland (as illustrated in Fig. 1).

Climate Data

Meteorological information were obtained from the Austrian Federal Ministry of Agriculture, Forestry, Environment and Water Management. We chose a dataset from November 1998 to October 1999 to cover both, an entire hydrological year and an heavy precipitation event. This heavy rainstorm occurred on the 20th of May 1999 and triggered several landslides in the study area. Former geomorphological studies (Schmaltz et al. 2016a, b) revealed that 14 landslides

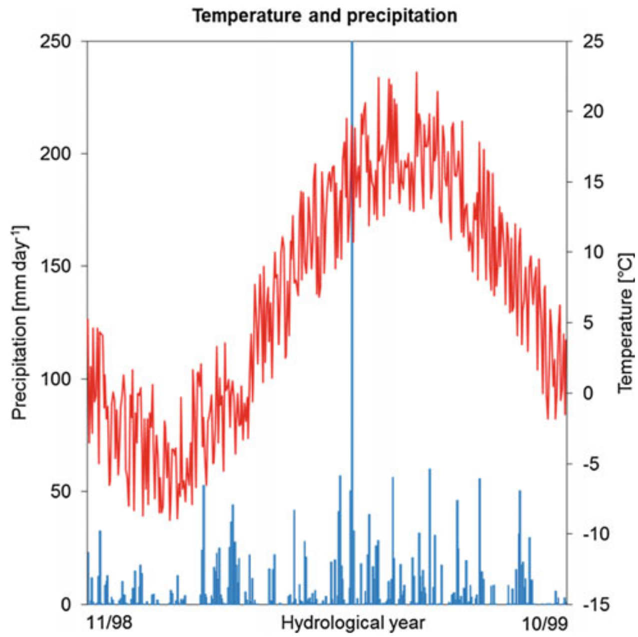

Fig. 2 Rainfall data for the hydrological year of November 1, 1998–October 31, 1999 (365 days). Precipitation data were provided by the Austrian Federal Ministry of Agriculture, Forestry, Environment and Water Management. Synthetic daily temperature was estimated based on monthly temperature information of the study site

with an average scarp area size of ~64 m^2 were triggered within the extent of the investigated area.

We estimated daily temperature data based on monthly precipitation information with a daily standard deviation of the temperature of 2.5 °C. This was performed due to the existent temperature gradient and the high temperature differences along the whole slope section (Fig. 2).

Methodology

Slope Stability Modelling

The probability of failure was assessed using the coupled model STARWARS/PROBSTAB, developed by Van Beek (2002) for translational landslides. The model contains a hydrological component (STARWARS) and a geomechanic module (PROBSTAB). In the hydrological part, the volumetric moisture content for the distinguished soil layers and groundwater level are calculated dynamically and spatially distributed. The geomechanic part uses the simulated hydrological parameters to calculate Factor of Safety (FoS) values and the slope failure probability. STARWARS/PROBSTAB is written in pcrcalc, processed with the pcraster GIS and embedded within the convenient pcraster-python framework. This allows a straightforward manipulation of the model code.

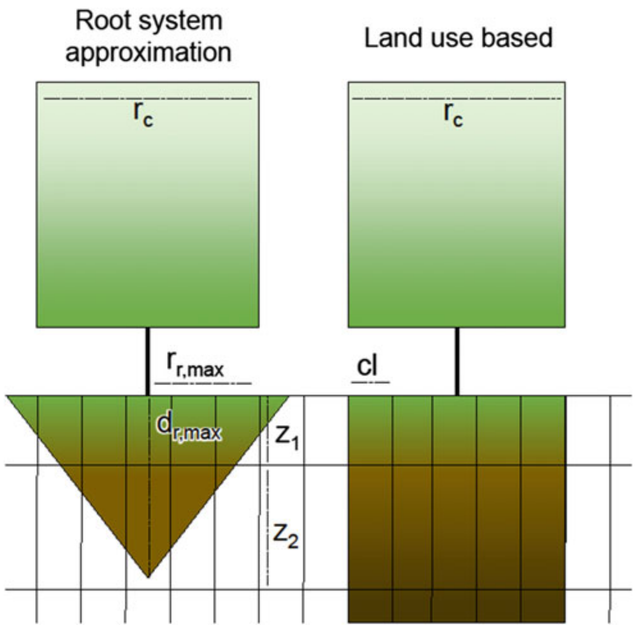

Fig. 3 2D-view of the applied root system approximation scheme in a raster environment. Where r_{c1} [m] is the diameter of the canopy, $r_{r,max}$ [m] is the maximum radius of the root system, $d_{r,max}$ [m] is the maximum depth of the root system, z_1 and z_2 [both m] are depths of soil layer 1 and 2 respectively and cl [m] is the length of a raster cell

No measured data of soil moisture content or groundwater level for validation of the modelling output were available for the chosen period. Thus, we primarily used the probability of failure and changes in volumetric soil moisture contents to compare three different scenarios:

(i) Scenario 1: The area without any vegetation cover.
(ii) Scenario 2: The study area is covered with vegetation—either forest that was assigned as a dense mixed forest (see Table 1) and grassland (land use based).
(iii) Scenario 3: Root system approximation was performed on areas that were assigned as forests. Not-forested areas were considered as sealed or grassland (see Fig. 1).

Schmaltz et al. (2016a) performed similar scenario analyses like those mentioned in bullet point i) and ii) on the different scales, for a greater area ($\sim$12 km^2) and lower resolution (10 × 10 m raster). Three test locations were defined to determine both differences in the soil moisture fluctuations of the three distinguished soil layers and the slope failure probability. Therefore, two spots were chosen under a forest cover (location 1 and 3) and in a none forested area (location 2) (see Fig. 8). A landslide was triggered at

Fig. 4 Changes of volumetric moisture content (y-axis; in % of respective maximum) of layer 1 (*top row*), layer 2 (*mid row*) and layer 3 (*bottom row*) for time steps (x axis; days) 175–225. The colored lines show the different test locations. *Black* location 1, *cyan* location 2, *magenta* location 3

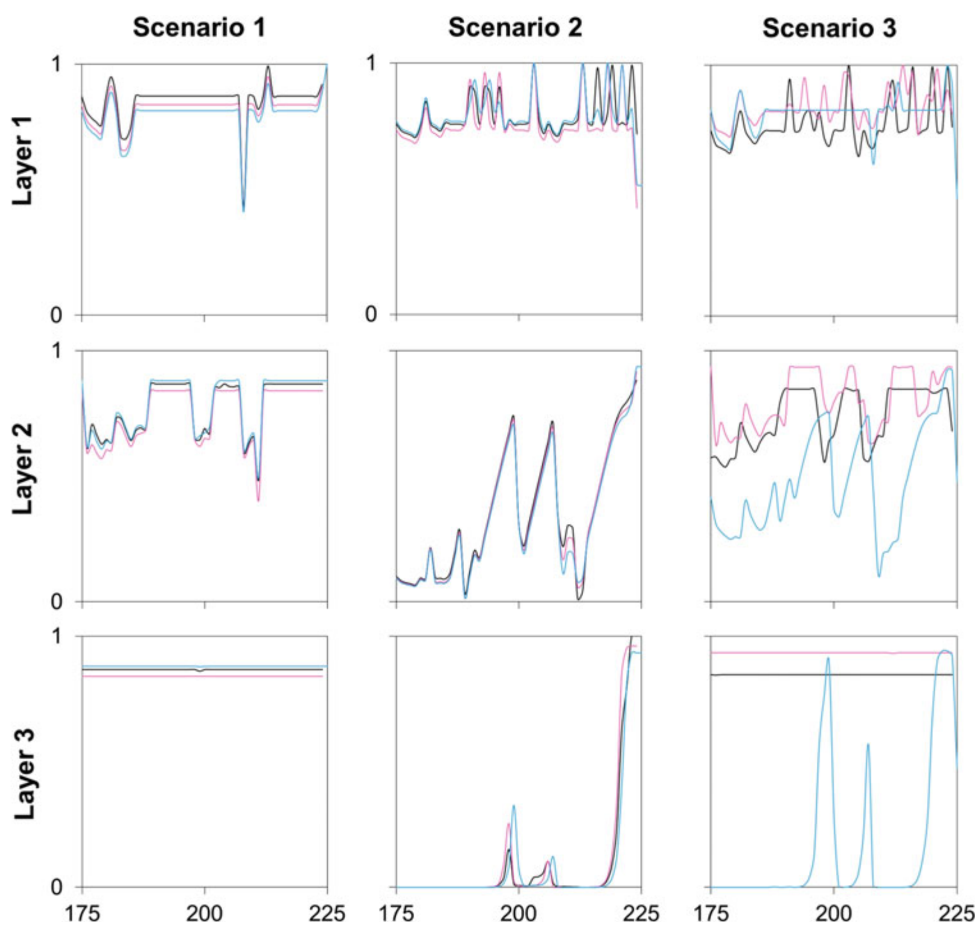

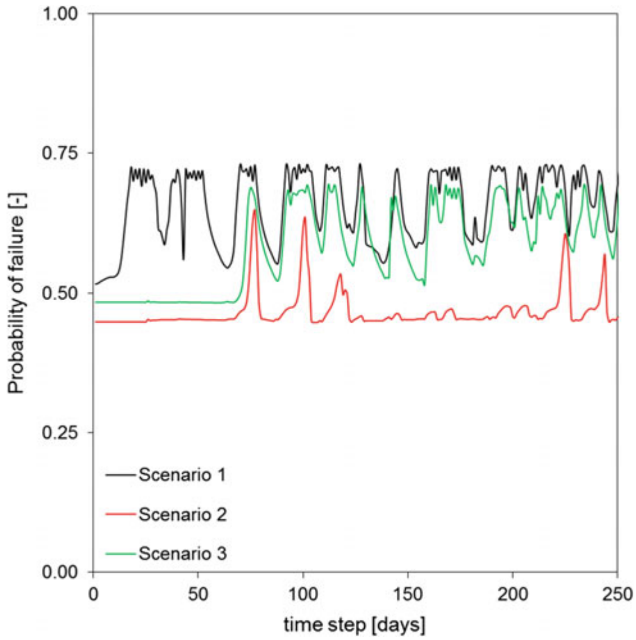

Fig. 5 Slope failure probability (Pf) at test location 1. Location 1 was located in the forest during the modelled hydrological year, however, deforested after a landslide event (c.f. Fig. 8)

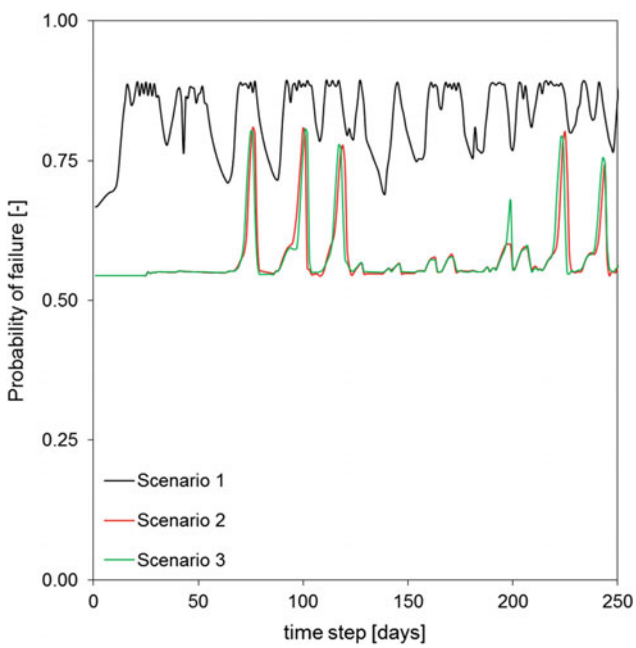

Fig. 6 Slope failure probability (Pf) for a not-forested area (location 2)

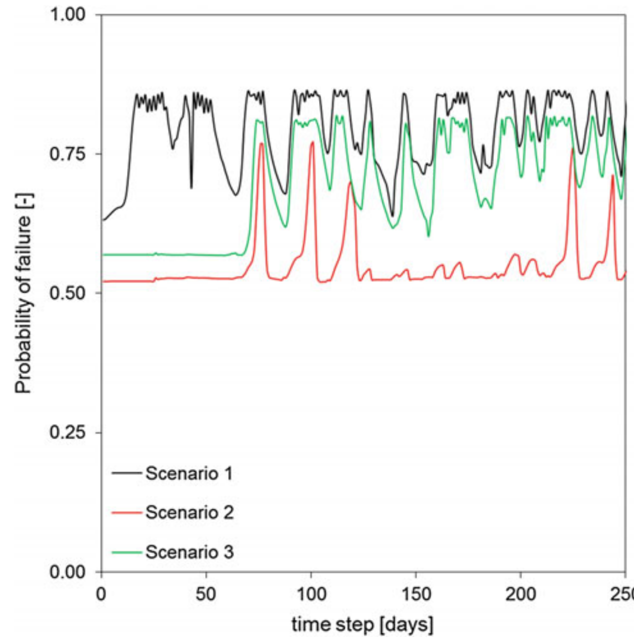

Fig. 7 Slope failure probability (Pf) for a forested area (location 3)

location 1, whereas the other two test locations appeared to remain stable.

Root System Approximation

Within scenario 3 we assumed that roots are distributed around the trunk of a tree with fixed maximum depth and distance. Both, distance and depth depend on tree species, soil type, nutrient and water availability as well as on climatic conditions (Sidle and Ochiai 2006; Thomas and Pollen-Bankhead 2008, Ghestem et al. 2012). For simplification, it is assumed that the maximum rooting distance around the trunk decreases with depth. Thus, the approximated rooted zone forms a cone shaped solid with variable ratios between maximum radius and maximum depth for certain rooting systems (Fig. 3).

Parameterization and Calibration

Soils

To carve out the effect of different vegetation covers, geotechnical soil parameter were kept constant for the whole

Table 1 Input-data of vegetation coverage for the modelled scenarios

Scen.	C_r (kPa)	Int. loss (m)	K_c (–)
1	0	0	0
2	4	4.5	1
3	4	4.5	1

*Scen. = Scenario; c_r = root cohesion; Int. loss = interception loss; K_c = cropfactor

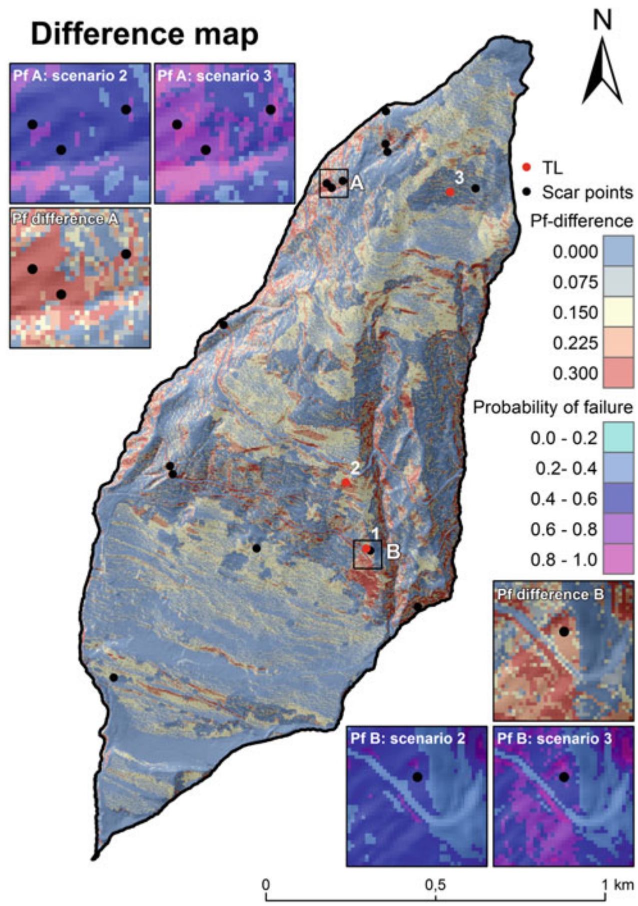

Fig. 8 Difference map between Pf-maps of scenario 3 and 2. Detailed views of Pf-maps and the Pf-difference for two representative areas A and B are provided in the *upper left* and the *lower right* corner of the figure. Moreover, landslides that were triggered 1999 are represented as scar points (*black*). Test locations (TL) that reflect Pf values (c.f. Figs. 5, 6, and 7) and volumetric soil moisture contents of the three soil layers (c.f. Fig. 4) are given as *red dots*

study area. Three different soil layers z_i with distinct geotechnical properties were distinguished. Geotechnical soil parameters (dry bulk density [γ], internal friction angle [Φ] and soil cohesion [c_r] at shear plane) used in the modelling procedure were set to uniform values for all three soil layers in the whole study site: $\gamma = 25.3$ kN m^{-3}, $\Phi = 35°$, $c_r = 2$ kPa.

A simplified version of a generic soil depth prediction model of Pelletier and Rasmussen (2009) was used to estimate soil depth:

$$z = \frac{h_0}{\sqrt{1 + \left|\frac{\partial z}{\partial x}\right|^2}} \ln\left(\frac{P_0}{U}\sqrt{1 + \left|\frac{\partial z}{\partial x}\right|^2}\right) \qquad (1)$$

where h_0 is the soil thickness [m] at which bedrock lowering falls of 1/e of its maximum value, P_0/U is the relation between the maximum lowering rate on a flat surface and the rock uplift rate. According to Pelletier and Rasmussen (2009) and Roering (2008) we used $\cos(\theta)$ for $1/\sqrt{(1 + |\partial z/\partial x|^2)}$ to express the topographic controls in terms of the slope normal coordinate direction z and its derivatives. The ratio P_0/U was neglected and kept as 1. Based on analysis in former studies, h_0 was set to 0.5 m (Heimsath et al. 1999, 2001). For the modelling procedure, we assumed the following percentages of thickness of each layer towards total depth based on field observations: layer 1 = 20% (topsoil), layer 2 and 3 = 2 × 40%.

Vegetation

To determine the effects of root reinforcement solely, the canopy cover of the trees and the maximum canopy interception storage was kept constant for forested areas (Table 1). Distribution of cohesion values within the root systems were not considered. Thus, we assumed a root cohesion value of 4 kPa for both scenarios with vegetation on all areas that are depicted as forested.

Usually, the cropfactor is obtained by considering time intervals between wetting events (e.g. rainfall, snowmelt), evaporation power of the atmosphere and the magnitude of the wetting event. For our study, we set Kc = 1, since this is a recommended value used for mixed and conifer forests (Allen et al. 1998).

The root fraction of a distinct soil layer z_i was calculated according to Eq. 2:

$$rootfrac(z_i) = \frac{\int_0^{z_{\max}} \frac{r_{\max}^2}{z_{\max}^2}\pi x^2 dx - \int_{zi}^{z_{\max}} \frac{r_i^2}{z_{\max}^2}\pi x^2 dx}{\int_0^{z_{\max}} \frac{r_{\max}^2}{z_{\max}^2}\pi x^2 dx} \qquad (2)$$

where z_i is the thickness of the soil layer [m], r_{max} [m] and z_{max} [m] are the maximum extent of the root system in lateral and vertical direction, respectively.

Results and Discussion

Figure 4 shows the changes of volumetric moisture content in soil layers 1–3 for all modelled scenarios and test locations. It is clearly recognizable that scenario 1 and 2 show quite similar changes in volumetric moisture content throughout all test locations. Whereas, scenario 3 exhibits patterns of both forests and areas with no vegetation cover.

This might be explained by the fact that the approximated root systems of scenario 3 do not cover as much of the soil column compared to scenario 2. In this regard, it is possible that the cone-shaped root systems do not reach the lithic boundary or even soil layer 3. Therefore, some locations show fluctuations of moisture content that are similar to conditions observed for unvegetated areas—particularly when the deeper soil layers 2 and 3 are considered (see Fig. 4, scenario 3). This moreover effectuates the course of pf-values over all time steps.

Generally, pf-values of the scenarios that include vegetation cover (2 and 3) can be clearly distinguished from those of scenario 1 (without vegetation cover) at all observed locations. Location 1 shows quite diverse reactions of slope failure probability (pf) values in the modelling output (Fig. 5). This forested location shows an immediate reaction on precipitation input for scenario 1 (no vegetation cover) at the first time steps and a resulting increase of pf-values to ~ 0.82. Scenario 2 and 3 show a significant rise of pf-values from time step 70, which depicts the end of the winter season and thus freezing conditions. However, for all locations, the probability of failure drops rapidly for scenario 2 between time steps 120 and 125 and is evened out until time step 220.

In contrast, the model output of scenario 3 shows a highly erratic pf-curve between time step 70 until the end of the model run at the forested locations 1 and 3.

Pf-curves of scenario 2 and 3 show similar courses for the whole modelled period at the non-forested location 2. However, scenario 3 exhibits a significantly higher peak at time step 200 than scenario 2. Time step 200 represents the high precipitation event at the 20th of May 1999. This finding indicates the effect of different vegetation input parameters on non-vegetated locations and a stronger reaction of the system when root distribution is decreased within the soil column.

The difference map of scenario 2 and 3 shows the spatial discrepancies of slope failure probability distribution between those models that include spatial information on the root system (Fig. 8). The map highlights that particular at areas where actual slope failures occurred, scenario 2 (land cover based approximation) tends to decisively overestimate the stabilizing impact of vegetation (detail views of locations A and B in Fig. 8).

Conclusion

In this study, we showed the effect of geometrical root system approximations on the dynamic hydromechanical slope stability model STARWARS/PROBSTAB. Three different land cover scenarios were compared: (1) the study area without vegetation cover; (2) the root system of forested areas are represented by the raster cell size and the depth of the soil column; (3) the root systems are geometrically approximated as a cone with distinct radius and depth emanating from the location of the tree stem. Soil depth was estimated with a simplified sine-cosine relation derived from generic soil depth prediction model of Pelletier and Rasmussen (2009). Geotechnical parameters as well as surface vegetation input (e.g. canopy coverage, interception capacity, etc.) were considered as constant for the whole modelled area. All scenarios were applied in a small study area in Vorarlberg, Austria.

The results show that the decision on how roots are spatially represented within a physically-based slope stability model (e.g. land cover based vs. cone-shaped approach) affects the modeling outcomes considerably. Scenario 2 and 3 give similar reactions of soil moisture fluctuations and slope failure probability on precipitation input—particularly in not vegetated areas. However, there are significant differences in forested areas recognizable. The model output of scenario 3 shows a much stronger reaction than scenario 2 and appears to align to pf-values of scenario 1 (no vegetation). It is assumed that scenario 3 primarily represents the stabilizing effect of root systems rather in the topsoil layer and thus shows similar patterns like scenario 2. In contrast, deeper soil layers show patterns of no vegetation coverage or a highly reduced vegetation impact respectively. This might be explained by the smaller volume that represents the rooted zone and thus a decreased root fraction for deeper layers of a respective soil column. First visual comparison (as shown in Fig. 8) suggests that, scenario 3 might reproduce slope failures more accurately that actually occurred during the modelled period. Hence, we expect that geometrical root system approximation is able to represent the hydrological and mechanical properties of roots more reliable in physically based models.

However, a drawback of our approach is the lack of quantitative evidence for its reliability due to the absence of measured data for validation. Moreover, tree locations and thus tree stand densities were estimated randomly for the forested areas, which produces a high uncertainty in the accuracy of root fraction calculation. In this context, it is expected that the envisaged inclusion of information based on highly resolved LiDAR data is able to decrease this uncertainty. The implementation of these airborne laser scanning data (ALS) could provide detailed information about vegetation on the surface from which subsurface biomass (e.g. roots) could be estimated more precisely. Moreover, the results outputs of this study open opportunities for better root system approximations (e.g. rotation ellipsoids) or the implementation of hydrological effects (e.g. water uptake capacity).

Acknowledgements We would like to thank the Federal State of Vorarlberg for providing remote sensing data and the Digital Elevation Model. Moreover, we thank our project partners of the BioSLIDE-project, Di Wang, Markus Hollaus and Norbert Pfeifer as well as the Torrent and Avalanche Control in Austria for supporting this study with valuable information and their expertise.

References

Allen RG, Pereira LS, Raes D, Smith M (1998) Crop evapotranspiration—guidelines for computing crop water requirements—FAO irrigation and drainage paper 56. FAO—Food and Agriculture Organization of the United Nations. Rome

Danjon F, Barker DH, Drexhage M, Stokes A (2002) Using three-dimensional plant root architecture in models of shallow-slope stability. Ann Bot 101(8):1281–1293

Fan C-C, Chen Y-W (2008) Role of roots in the shear strength of root-reinforced soils with high moisture content. Ecol Eng 33 (2):157–166

Fan C-C, Chen Y-W (2010) The effect of root architecture on the resistance of root-permeated soils. Ecol Eng 36(6):813–826

Friebe G (2013) Steine und Landschaft—Zur Geologie der Jagdberggemeinden. In: Naturmonographie Jagdberggebeinden. Dornbirn: inatura Erlebnis Naturschau:41–52

Genet M, Kokutse N, Stokes A, Fourcaud T, Cai X, Ji J, Michovski SB (2008) Root reinforcement in plantations of cryptomeria japonica D. Don. effect of tree age and stand structure on slope stability. For Ecol Manage. 256(8):1517–1526

Ghestem M, Sidle RC, Stokes A (2011) The influence of plant root systems on subsurface flow: implications for slope stability. Bioscience 61(11):869–879

Greenway DR (1987) Vegetation and slope stability. In: Anderson MG, Richards KS (eds) slope stability: geotechnical engineering and geomorphology. Wiley and Sons, New York, pp 187–230

Heimsath AM, Dietrich WE, Nishiizumi K, Finkel RC (1999) Cosmogenic nuclides, topography, and the spatial variation of soil depth. Geomorphology 27(1):151–172

Heimsath AM, Dietrich WE, Nishiizumi K, Finkel RC (2001) Stochastic processes of soil production and transport: erosion rates, topographic variation and cosmogenic nuclides in the Oregon Coast range. Earth Surf Process Land 26(5):531–552

Imaizumi F, Sidle RC, Kamei R (2008) Effects of forest harvesting on the occurrence of landslides and debris flows in steep terrain of central Japan. Earth Surf Process Land 33(6):827–840

Meng W, Bogaard T, Van Beek LPH (2014) How the stabilizing effect of vegetation on a slope changes over time: a review. Landslide Sci Safer Geoenvironment 1:363–372

Montgomery DR, Schmidt KM, Greenberg HM, Dietrich WE (2000) Forest clearing and regional landsliding. Geology 28(4):311–314

Papathoma-Köhle M, Glade T (2013) The role of vegetation cover change for landslide hazard and risk. In: Renaud G, Sudmeier-Rieux K, Estrella M (eds) The role of ecosystems in disaster risk reduction. UNU-Press, Tokyo, pp 293–320

Pelletier JD, Rasmussen C (2009) Geomorphologically based predictive mapping of soil thickness in pland watersheds. Water Res Res 45(9):1–15

Pollen N, Simon A (2005) Estimating the mechanical effects of riparian vegetation on stream bank stability using a fiber bundle model. Water Resour Res 41(7):1–11

Roering JJ (2008) How well can hillslope evolution models “explain” topography. Geol Soc Am Bull 120(9–10):1248–1262

Ruff M, Czurda K (2008) Landslide susceptibility analysis with a heuristic approach in the Eastern Alps (Vorarlberg, Austria). Geomorphology 94(3):314–324

Schmaltz E, Steger S, Bell R, Glade T, Van Beek LPH, Bogaard T, Wang D, Hollaus M, Pfeifer N (2016a) Exploring possibilities of including detailed ALS derived biomass information into physically-based slope stability models at regional scale. In: Aversa et al. (eds) Landslides and engineered slopes. Experience, theory and practice,pp 1807–1815

Schmaltz E, Steger S, Bell R, Glade T, Van Beek LPH, Bogaard T, Wang D, Hollaus M, Pfeifer N. (2016b) Evaluation of shallow landslides in the Northern Walgau (Austria) using morphometric analysis techniques. Procedia Earth and Planet Sci. Article in press

Schmid I, Kazda M (2002) Root distribution of Norway spruce in monospecific and mixed stands on different soils. For Ecol Manage 159(1–2):37–47

Schwarz M, Cohen D, Or D (2012) Spatial characterization of root reinforcement at stand scale. Theory and case study Geomorphol 171:190–200

Schwarz M, Lehmann P, Or D (2010) Quantifying lateral root reinforcement in steep slopes—from a bundle of roots to tree stands. Earth Surf Process Land 35(3):354–367

Sidle RC (1991) A conceptual model of changes in root cohesion in response to vegetation management. J Environ Qual 20(1):43–52

Sidle RC, Ochiai H (2006) Landslides: processes, prediction, and land use. Water resources monograph 18, American Geophysical Union, Washington D C

Sidle RC, Pearce AJ, O’Loughlin CL (1985) Hillslope stability and land use. Water Resources monograph 11, American Geophysical Union, Washington D C

Stokes A, Douglas GB, Fourcaud T, Giadrossich F, Gillies C, Hubble T (2014) Ecological mitigation of hillslope instability. Ten key issues facing researchers and practitioners. Plant Soil 377(1–2):1–23

Stokes A, Norris JE, Van Beek LPH, Bogaard T, Cammeraat E, Michovski SB (2008) How vegetation reinforces soil on slopes. In: Norris JE et al. (eds) Slope stability and erosion control: ecotechnological solutions. Springer, pp 65–118

Thomas RE, Pollen-Bankhead N (2010) Modelling root-reinforcement with a fibre-bundle model and Monte Carlo simulation. Ecol Eng 36 (1):47–61

Tilch N (2014) Identifizierung Gravitativer Massenbewegungen mittels multitemporaler Luftbild-auswertung in Vorarlberg und angrenzender Gebiete. Jahrbuch der Geologischen Bundesanstalt 154(1–4):21–39

Van Beek LPH, Wint J, Cammeraat L, Edwards JP (2007) Observation and simulation of root reinforcement on abandoned Mediterranean slopes. In: Stokes A et al. (eds) Eco- and ground bio-engineering: the use of vegetation to improve slope stability. Springer, pp 91–109

Ziemer, RR (1981) The role of vegetation in the stability of forested slopes. In: Proceedings of the International Union of Forestry Research Organizations, XVII World Congress, vol 1. pp 297–308